Free-Energy Landscapes of Ion-Channel Gating Are Malleable: Changes in the Number of Bound Ligands Are Accompanied by Changes in the Location of the Transition State in Acetylcholine-Receptor Channels†

Claudio Grosman*

Department of Molecular and Integrative Physiology and Center for Biophysics and Computational Biology, University of Illinois at Urbana-Champaign, Urbana, Illinois 61801

Received August 11, 2003; Revised Manuscript Received October 15, 2003

ABSTRACT: Acetylcholine-receptor channels (AChRs) are allosteric membrane proteins that mediate synaptic transmission by alternatively opening and closing ("gating") a cation-selective transmembrane pore. Although ligand binding is not required for the channel to open, the binding of agonists (for example, acetylcholine) increases the closed ⇌ open equilibrium constant because the ion-impermeable → ion-permeable transition of the ion pathway is accompanied by a low-affinity → high-affinity change at the agonist-binding sites. The fact that the gating conformational change of muscle AChRs can be kinetically modeled as a two-state reaction has paved the way to the experimental characterization of the corresponding transition state, which represents a snapshot of the continuous sequence of molecular events separating the closed and open states. Previous studies of fully (di) liganded AChRs, combining single-channel kinetic measurements, site-directed mutagenesis, and data analysis in the framework of the linear free-energy relationships of physical organic chemistry, have suggested a transition-state structure that is consistent with channel opening being an asynchronous conformational change that starts at the extracellular agonist-binding sites and propagates toward the intracellular end of the pore. In this paper, I characterize the gating transition state of unliganded AChRs, and report a remarkable difference: unlike that of diliganded gating, the unliganded transition state is not a hybrid of the closed- and open-state structures but, rather, is almost indistinguishable from the open state itself. This displacement of the transition state along the reaction coordinate obscures the mechanism underlying the unliganded closed ⇌ open reaction but brings to light the malleable nature of free-energy landscapes of ion-channel gating.

The muscle acetylcholine-receptor channel (AChR)[1] is the neurotransmitter-gated ion channel that mediates neuromuscular synaptic transmission in vertebrates (*1*). Although the structure of this large pentameric transmembrane protein (∼470 residues per subunit) is not known with atomic resolution, a wealth of structural information exists, mainly from mutational studies, affinity labeling, chemical modification of specific residues, electron microscopy, and crystallography (reviewed in ref *2*). As is the case for any other allosteric protein, the dynamic behavior of this receptor channel can be understood in the framework of thermodynamic cycles, with conformational changes and ligand-binding events as the elementary steps (*3*−*5*). Thus, the AChR can adopt a variety of different conformations that can interconvert (closed, open, and desensitized "states"), and each conformation has a distinct ligand-binding affinity (low affinity in the closed state and high affinity in the open and desensitized states) and a particular "catalytic efficiency" (ion-impermeable in the closed and desensitized states, and ion-permeable in the open state). To meet the physiological requirement of a small closed ⇌ open ("gating") equilibrium constant for the unliganded receptor, and a large gating equilibrium constant for the ACh-diliganded receptor, the affinity of the AChR for ACh must be higher in the open than in the closed conformation (*4*−*6*). This follows from the notion that the equilibrium constants governing the different reaction steps (ligand binding and gating) of these cyclic reaction schemes are constrained by the principle of detailed balance.

Hence, irrespective of whether the receptor is diliganded, monoliganded, or unliganded, two changes must take place in going from the closed state (low ligand affinity and ion-impermeable) to the open state (high ligand affinity and ion-permeable): (a) the pore becomes permeable to ions, and (b) the transmitter-binding sites, 50 Å away from the pore domain (*7*), increase their affinity for the ligand (with the reverse changes taking place during closing). The apparent lack of stable intermediates between the closed and open conformations, inferred from kinetic modeling of the diliganded-gating reaction (*8*), suggests that these two changes occur as a result of a one-step, global conformational change. The question, then, arises as to whether this concerted conformational change proceeds synchronously (i.e., every

† This work was supported by grants from the National Institutes of Health (NS042169 to C.G. and NS23513 to Anthony Auerbach).

* To whom correspondence should be addressed. Phone: (217) 244-1736. Fax: (217) 333-1133. E-mail: grosman@life.uiuc.edu.

[1] Abbreviations: AChR, acetylcholine receptor channel; ACh, acetylcholine; M2, second transmembrane segment; M3, third transmembrane segment.

10.1021/bi0354334 CCC: $25.00
Published on Web 11/21/2003

residue of the protein moves "in unison") or asynchronously (i.e., following a sequence of events; *9*) and, if the latter were the case, whether multiple, a few, or just one sequence of events is actually traversed by the channel to "connect" the end states.

Analysis of the correlation between rate and equilibrium constants of gating in diliganded AChRs has allowed us to address some of these issues by probing the structure of the transition state (*8*, *10*−*12*), that is, the intermediate species between the end states of a one-step reaction that can be most easily studied. Interpretation of these results in the framework of the classical rate−equilibrium free-energy relationships of physical organic chemistry (*13*, *14*) revealed that AChR diliganded gating is a highly asynchronous reaction, and suggested that the transition-state ensemble is quite homogeneous, as if the crossing of the energy barrier were confined to a narrow pass at the top of the energy landscape. In the opening direction, the conformational rearrangement that leads to the low- to high-affinity change at the extracellular binding sites precedes the conformational rearrangement of the pore that renders the channel ion-permeable. This propagated global conformational change, which we have referred to as a "conformational wave" (*11*), must reverse during channel closing so that closing starts at the pore and propagates all the way to the binding sites.

It is not at all obvious why the *diliganded*-gating conformational change starts at the binding sites when the channel opens, nor even why the conformational change propagates at all through the receptor, instead of taking place synchronously throughout the protein. Is there any correlation between the location of the domain that binds agonist and the location of the initiation site for the opening conformational change? Could the latter have started from the intracellular end of the pore, for example, and have propagated to the (extracellular) transmitter-binding sites? What difference does it make to be liganded or unliganded as far as the mechanism of the gating conformational change is concerned? To address these issues, I set out to explore the mechanism of gating in *un*liganded AChRs by probing the structure of the corresponding transition state using kinetic measurements, site-directed mutagenesis, and the concepts of rate−equilibrium free-energy relationships and Φ-value analysis.

Briefly, a Φ-value can be assigned to any position in the protein by estimating the slope of a "Brönsted plot" [2] [log(gating rate constant) versus log(gating equilibrium constant)] where each point in the plot corresponds to a different amino acid substitution at that given position. More coarse-grained Φ-values can also be obtained by using different agonists or different transmembrane potentials, for example, as a means of altering the rate and equilibrium constants of gating. Very often, rate−equilibrium plots are linear, and $0 < \Phi < 1$. A value of $\Phi = 0$ suggests that the position in question (in the case of a mutation series) experiences a closed-state-like environment at the transition state, whereas a value of $\Phi = 1$ suggests an open-state-like environment. A fractional

[2] "Brönsted plot" is actually a misnomer. In the original work (*15*), the plotted rate and equilibrium constants correspond to two *different* reactions. However, the name is so widely used now to designate the rate−equilibrium type of plot used in this paper (rate and equilibrium constants correspond to the same reaction) that I decided to keep it.

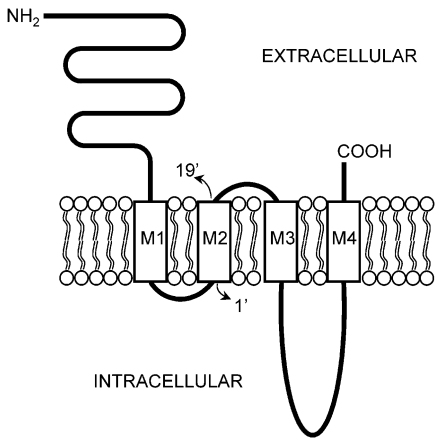

FIGURE 1: Putative threading pattern of an AChR subunit through the membrane. This pattern is thought to be conserved throughout the superfamily of Cys-loop receptor subunits (which includes, in vertebrates, the subunits that form acetylcholine nicotinic receptors, serotonin type 3 receptors, glycine receptors, and γ-aminobutyric acid type A and type C receptors). The M2 domain is thought to be a transmembrane, mostly α-helical segment with 19 intramembrane residues (referred to as 1′ to 19′, from the intracellular to the extracellular end). Five M2 segments, each contributed by a different subunit of the pentameric receptor channel, form most of the lining of the membrane pore (*2*). An alternative threading pattern with M1 having as many as three nonhelical transmembrane passes has been recently proposed (*19*). This discrepancy, however, does not compromise the conclusions of this work. The adult form of the muscle-type AChR is formed by four different subunits (α, β, δ, and ϵ) in an $\alpha_2\beta\delta\epsilon$ stoichiometry.

Φ-value suggests an environment that is intermediate between those experienced in the closed and open states (*16*).

Earlier results indicated that the Φ-values obtained by varying the transmembrane potential are different in diliganded and unliganded AChRs. These Φ-values, which are a measure of the closed-state-like versus open-state-like character of the channel's voltage-sensing elements at the transition state, are 0.070 ± 0.060 in diliganded receptors (*17*) and 1.025 ± 0.053 in unliganded AChRs (*11*, *18*). The present study reveals that residues at the transmitter-binding sites (Figure 1), the extracellular loop that links the second (M2) and third (M3) transmembrane segments (M2−M3 linker), and the upper and lower half of M2, which during diliganded gating have Φ-values of ∼1 (*11*), ∼0.7 (*10*), ∼0.35 (*8*, *11*, *12*), and ∼0 (*12*), respectively, also have Φ-values very close to 1 during unliganded gating. This generalized shift in Φ-values suggests that the diliganded → unliganded perturbation deforms the energy landscape of gating in such a way that the "new" transition state occurs very close to the open state, to such an extent that all tested positions experience an open-state-like environment at the transition state of unliganded gating. Thus, the transition state occurs so "late" (i.e., so close to the open state) that its inferred structure does not provide any clues as to the *intermediate* stages of this reaction.

Hence, the mechanism of unliganded gating remains obscure. The change in the position of the transition state along a reaction coordinate, as a result of perturbations to the energy landscape, is a very well-known phenomenon in organic chemistry (e.g., refs *20*−*26*) and protein folding (e.g., refs *27*−*34*). In this paper, I show that this phenomenon can also take place in the case of allosteric transitions and, therefore, that the structure of the transition state of a global

conformational change need not be fixed; rather, it can change depending on the experimental conditions.

EXPERIMENTAL PROCEDURES

Mutagenesis and Expression. Mouse cDNA clones corresponding to the α, *β*, *δ*, and *ϵ* subunits of the muscle AChR were generously provided by Dr. S. M. Sine (Department of Physiology and Biophysics, Mayo Foundation, Rochester, MN) in the CMV-based expression vector pRBG4 (*35*), and are described in ref *36*. The mutants αY93F, αY190W, and αD200N in pRBG4 were also a generous gift of Dr. S. M. Sine. Mutations αL251A, αS269I, *β*T265S, *δ*L265T, *δ*S268A, *δ*S268I, *δ*S268N, and *δ*S268Y were engineered using the QuikChange site-directed mutagenesis kit protocol (Stratagene, La Jolla, CA). Mutations *δ*S268T and *ϵ*T264S were engineered by overlap PCR (*37*). All constructs were confirmed by dideoxy sequencing.

Human embryonic kidney fibroblast cells (HEK 293) were transiently transfected using a calcium phosphate precipitation protocol. A total of 3.5 *μ*g of cDNA per 35 mm culture dish in the ratio 2:1:1:1 (α:*β*:*δ*:*ϵ*) was applied to the cells for approximately 20 h, after which the culture medium was changed. Electrophysiological recordings started ∼30 h later.

Cell-Attached Single-Channel Recordings. Recordings were performed in the cell-attached patch configuration (*38*) at ∼22 °C. The bath solution was Dulbecco's phosphate-buffered saline (137 mM NaCl, 0.9 mM $CaCl_2$, 2.7 mM KCl, 1.5 mM KH_2PO_4, 0.5 mM $MgCl_2$, and 8.1 mM Na_2HPO_4, pH 7.3). The pipet solution was either a K^+/HEPES saline (142 mM KCl, 5.4 mM NaCl, 1.8 mM $CaCl_2$, 1.7 mM $MgCl_2$, 10 mM HEPES/KOH, pH 7.4) or the Na^+/phosphate saline also used as the bath solution. Patch pipets pulled from borosilicate capillaries were coated with Sylgard (Dow Corning Co., Midland, MI) and fire-polished. Pipet resistances ranged between 7.5 and 12.5 MΩ. Cell-attached single-channel currents were recorded using an Axopatch 200B (Axon Instruments, Foster City, CA) at a bandwidth of 100 kHz, digitized at a frequency of 94.4 kHz (VR-10B, f_c = 37 kHz; Instrutech Corp., Port Washington, NY), and stored on videotape. For analysis, the recordings were transferred to a PC via either an Instrutech VR111 or a National Instruments PCI-MIO 16E-4 (National Instruments Corp., Austin, TX) digital interface, at a sampling frequency of 94.4 or 100 kHz, respectively. The pipet potential of the cell-attached patches was generally held at +65 mV, and the average single-channel current amplitude recorded in the different cell-attached patches was −6.45 pA. Given the value of 74.5 pS for the single-channel conductance of unliganded AChRs (*18*), a value of −6.45 pA corresponds to a transmembrane potential of ∼−87 mV.

Single-Channel Analysis. Single-channel data analysis was performed using QuB software (www.qub.buffalo.edu; *39*). Schematically, the data analysis consisted of three steps. First, the digitized recordings were visually inspected to identify and remove noisy sections and those containing simultaneous openings of two or more channels. The durations of these removed sections were kept, however, so that each recording remained as an uninterrupted stretch of time. Typically, >98% of the original recording "survived" this step. Second, the recordings were idealized using a hidden-Markov modeling procedure (recursive Viterbi algorithm; "SKM" in QuB software), which also estimates the current amplitudes (*40*). The bandwidth of the recordings prior to this idealization step was further reduced by filtering the data digitally. This final bandwidth ranged between DC-18 and DC-23 kHz. Third, the idealized series of dwell times were used to estimate the rate constants that, given a kinetic model, fit the data best. This was done by using an interval-based full-likelihood algorithm that includes an approximate solution to the missed-events problem ("MIL" in QuB software). Prior to this step, a consistent time resolution was imposed on the idealized open and shut intervals (the same for both) by considering all intervals shorter than a given value ("dead time") as belonging to the conductance of the flanking sojourns. A dead time of 25 *μ*s was used throughout.

Rate−Equilibrium Free-energy Relationships and Φ-Values. The end states of a chemical reaction (involving changes in either covalent or noncovalent bonds) can become stabilized or destabilized upon a perturbation, and the balance between these free-energy changes determines the magnitude and direction of the change in the equilibrium constant. However, given only the latter, nothing can be said about the changes in the underlying rate constants although, in many cases, an "extrathermodynamic" (*13*, *14*) relationship between rate and equilibrium constants holds for reactions that occur in one step. In the context of ion-channel gating

$$G^{\ddagger p} - G^{\ddagger} = \Phi(G^{\circ p}_{open} - G^{\circ}_{open}) + (1 - \Phi)(G^{\circ p}_{closed} - G^{\circ}_{closed}) \quad (1)$$

where $G^{\circ p}_{open} - G^{\circ}_{open}$, $G^{\circ p}_{closed} - G^{\circ}_{closed}$, and $G^{\ddagger p} - G^{\ddagger}$ denote the Gibbs free-energy changes upon perturbation experienced by the open state, the closed state, and the intervening transition state, respectively, and Φ is the weighting factor. The closer Φ is to 1 (or 0), the closer the free-energy change undergone by the transition state is to that undergone by the open (or closed) state. Thus, Φ is a measure of how open-state-like versus closed-state-like the sensitivity of the transition state's free energy is. Because this energetic resemblance must have a structural correlate (e.g., ref *41*), Φ also measures the extent to which the microenvironment of the perturbed region of the protein, at the transition state, structurally resembles that in the open state (with 1 − Φ measuring the "closedness" of the transition state). Hence, Φ provides an indication of reaction progress at the particular moment when the transition state occurs. Since every residue of the protein can be perturbed using site-directed mutagenesis, a residue-by-residue picture of the transition state can, in principle, be obtained in terms of the resemblance to either end state. Equation 1 can be rearranged into eqs 2 and 3,

$$\log \beta = \Phi \log \beta/\alpha + \log k_o \quad (2)$$

$$\log \alpha = (\Phi - 1) \log \beta/\alpha + \log k_o \quad (3)$$

which allow the estimation of Φ from experimentally estimated rate constants. *β* and α are the channel opening and closing rate constants, respectively, of the different members of a reaction series (e.g., a number of mutants differing only in the amino acid residue at a given position), k_o (the intrinsic gating rate constant, a constant value for each series) is the value of *β* and α when the equilibrium

constant is unity, and Φ (or Φ − 1) is the slope of the linear fit. Therefore, given a change in a reaction's equilibrium constant upon perturbation *and* the Φ-value corresponding to the perturbed region, the underlying forward and backward rate constants become uniquely determined, and can be analytically estimated even if they are, say, too fast to be measured.

RESULTS

To probe the structure of the transition state of the unliganded closed ⇌ open reaction in muscle AChRs, I performed a Brönsted type of analysis, of the sort typically done for the investigation of reaction mechanisms in organic chemistry (e.g., ref *42*), enzymology (e.g., ref *43*), protein folding (e.g., ref *44*), and, more recently, allosteric transitions (*5*, *11*, *45*−*47*) and RNA folding (e.g., ref *48*). More specifically, I made mutations to various parts of the AChR (Figure 1) as a means of generating receptor variants with different combinations of unliganded-gating rate and equilibrium constants, and analyzed the correlation between them. Thus, this approach turns out to be virtually identical to what is known, in the protein-folding field, as "protein-engineering Φ-value analysis", the staple fare of two-state protein-folding studies (e.g., ref *49*).

Unliganded-Gating Kinetics. The concept of rate−equilibrium free-energy relationships (see eqs 1−3 in the Experimental Procedures) applies to reactions that occur in a *single* kinetically distinguishable step. In our previous single-channel studies, we found evidence that AChR diliganded gating can, indeed, be modeled as a one-step isomerization because both closed- and open-interval durations are monoexponentially distributed (*8*). In the case of unliganded gating, however, establishing whether this is the case turned out to be impossible because the statistical distributions of open and shut intervals (in the context of this paper "shut" refers to intervals that represent sojourns in nonconductive states, irrespective of whether these correspond to closed or desensitized conformations of the channel) were complex and could not be interpreted physically. Moreover, adding to this complexity, the reaction scheme that fitted the data best varied from mutant to mutant, and even from patch to patch in cells expressing the same mutant.

Figures 2−4 show example single-channel traces, and the corresponding open- and shut-time distributions, for the M2−M3-linker mutant αS269I, and for the M2 9′ position mutants δL265T and αL251A, respectively. Depending on the experiment, up to three exponential components were needed to fit the distribution of unliganded open times. Regardless of the particular number, however, open lifetimes always "fell" into a well-defined category of brief (ten to a few hundred microseconds), intermediate (several hundred microseconds), or long (several milliseconds) duration. The brief type of opening was present in all patches, and in those cases where more open components were present, this brief type still accounted for the majority of openings (77% of all openings in these patches, on average). When two exponential components were required, either the brief and the intermediate or the brief and the long-lived types of openings were present. These long-lived openings, which, when present, were always the least frequent (9.5%, on average),

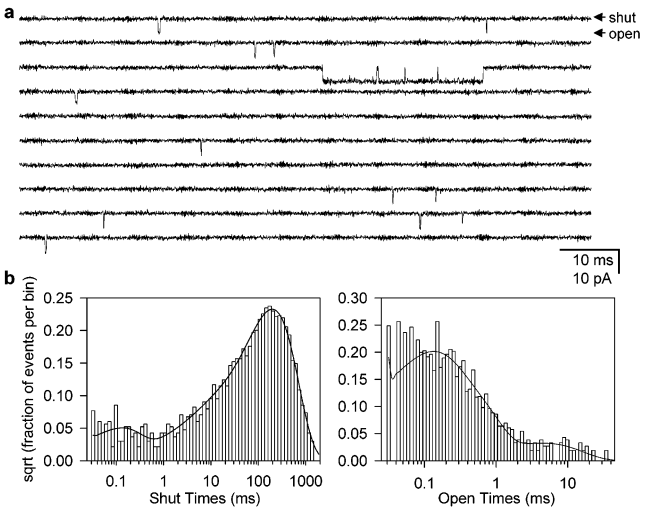

FIGURE 2: Continuous recording of single-channel inward currents and corresponding dwell-time histograms from unliganded αS269I AChRs. (A) Openings are downward deflections. For display purposes only, the bandwidth was reduced to 6 kHz. (B) Experimental dwell-time histograms and calculated density functions. The latter were computed from the rate-constant estimates (see legend to Figure 5), taking into account that a dead time of 25 μs was imposed on the idealized open and shut intervals. In this particular patch, the time constants (and areas) of the shut-time distribution were 99 μs (0.021), 124 μs (0.011), 7.6 ms (0.041), and 167 ms (0.927). For the open times, these were 95 μs (0.570), 280 μs (0.403), and 4.0 ms (0.027). The longest lived openings occurred in bursts of 1.8 openings, on average. In other words, 30% of these openings occurred as isolated events, 27% occurred as pairs of openings separated by one brief gap, 18% formed triplets containing two gaps, 11% came as quartets with three gaps, and so on.

were particularly striking as they occurred in "bursts" of (∼1.5) openings separated by short (<200 μs) gaps, a type of activity that is a hallmark of diliganded AChRs in the presence of low concentrations of ACh (<5 μM), in both the wild type (*50*) and "gain-of-function" mutants (*6*). However, I dismiss the idea that these openings reflect contamination of the recording system with cholinergic ligands. For example, in the case of the M2−M3-linker mutant, the only recording that displayed bursts of long-lived openings was obtained the same day, using the same dish of transfected cells, and using the same bath and pipet solutions as three other recordings that did not exhibit this type of activity. Also, I investigated the putative role of HEPES itself (present in the patch-pipet solution), as the ligand causing these openings, by replacing it with a mixture of phosphates (see the Experimental Procedures). Under these conditions, I recorded single-channel currents from two M2 9′ mutants (αL251A and δL265T), and found no correlation whatsoever between the presence of either pH-buffer system in the pipet solution and the occurrence of multiple open states.

The long-lived type of opening was not observed in recordings from wild-type AChRs, which, in most cases, displayed two open components (the brief and intermediate ones), in agreement with earlier observations made by Jackson (*51*). In fact, there appears to be a correlation between the incidence of long-lived openings and the location of the mutation in the receptor. Indeed, this type of opening was recorded in 28 out of a total of 31 patches containing AChRs mutated in M2, in only 1 out of 7 patches with receptors mutated in the M2−M3 linker, and in 0 out of 13

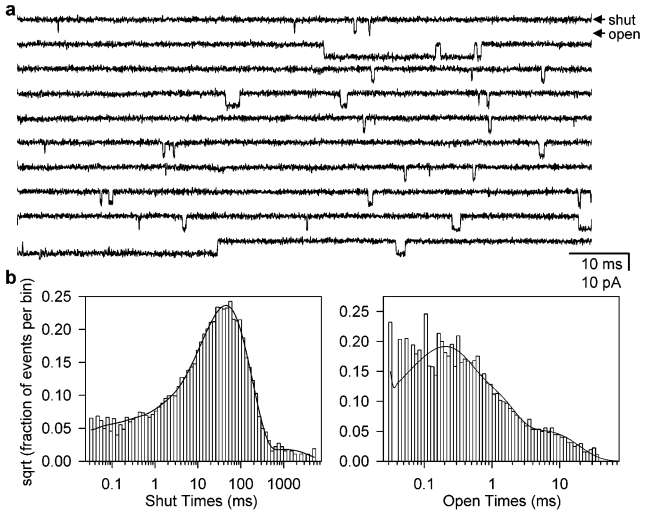

FIGURE 3: Continuous recording of single-channel inward currents and corresponding dwell-time histograms from unliganded δL265T AChRs. (A) Openings are downward deflections. For display purposes only, the bandwidth was reduced to 6 kHz. (B) Experimental dwell-time histograms and calculated density functions. The latter were computed from the rate-constant estimates (see the caption to Figure 5), taking into account that a dead time of 25 μs was imposed on the idealized open and shut intervals. In this particular patch, the time constants (and areas) of the shut-time distribution were 36 μs (0.009), 166 μs (0.025), 877 μs (0.038), 23 ms (0.250), 47 ms (0.667), 283 ms (0.009), and 2.0 s (0.001). For the open times, these were 149 μs (0.589), 600 μs (0.347), and 4.7 ms (0.064). The longest lived openings occurred in bursts of 1.7 openings, on average. In other words, 33% of these openings occurred as isolated events, 28% occurred as pairs of openings separated by one brief gap, 18% formed triplets containing two gaps, 10% came as quartets with three gaps, and so on.

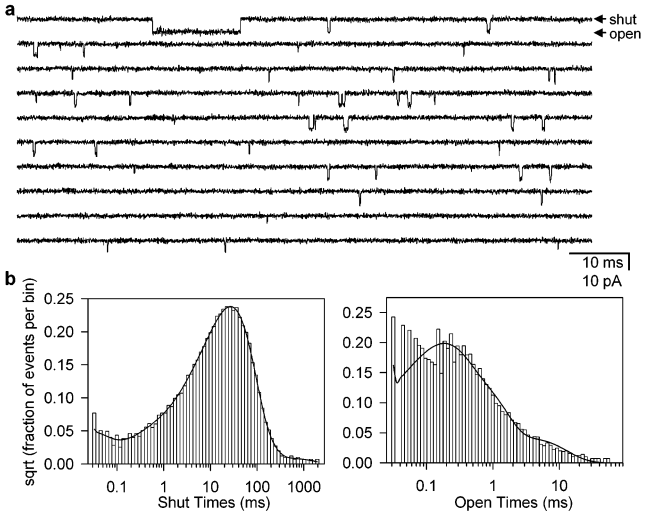

FIGURE 4: Continuous recording of single-channel inward currents and corresponding dwell-time histograms from unliganded αL251A AChRs. (A) Openings are downward deflections. For display purposes only, the bandwidth was reduced to 6 kHz. (B) Experimental dwell-time histograms and calculated density functions. The latter were computed from the rate-constant estimates (see the caption to Figure 5), taking into account that a dead time of 25 μs was imposed on the idealized open and shut intervals. In this particular patch, the time constants (and areas) of the shut-time distribution were 16 μs (0.006), 36 μs (0.006), 370 μs (0.008), 22 ms (0.923), 49 ms (0.056), and 382 ms (0.001). For the open times, these were 130 μs (0.583), 452 μs (0.379), and 3.1 ms (0.038). The longest lived openings occurred in bursts of 1.4 openings, on average. In other words, 54% of these openings occurred as isolated events, 29% occurred as pairs of openings separated by one brief gap, 11% formed triplets containing two gaps, 4% came as quartets with three gaps, and so on.

patches with AChRs bearing binding-site mutations. This suggests that these slow unliganded openings are favored by mutations in M2.

The grouping of consecutive openings in a burst is a typical observation in single-channel recordings from wild-type muscle AChRs in the presence of low concentrations of ACh (*50*). The openings within each burst are interpreted to arise from a receptor channel that is bound to a given pair of ACh molecules, and that opens and closes repeatedly until entry into long-lived desensitized states or ligand dissociation (from either the closed or the open conformation) occurs (*6*). Thus, the unexpected observation that mutant AChRs can open in a burst-like manner even when unliganded suggests the existence of an additional mechanism for the channel to generate bursts of openings, and calls for further investigation. It is not clear whether this multiplicity of open states reflects the existence of a heterogeneous channel population (receptors with different extents of posttranslational modifications, for example) or the existence of different open conformations that are made accessible to the unliganded AChR by mutations. It is curious that the statistical distribution of open times in unliganded AChRs is more complex than that in diliganded receptors.

The distribution of shut times was also far from straightforward, consisting of up to six exponential components in some patches, and it was much less predictable than the distribution of open times. Again, it is not clear what these multiple shut states represent, but they may well reflect the existence of a variety of desensitized conformations that mutant AChRs can visit even in the absence of ligand, and not necessarily the existence of multiple closed states. Because it was impossible to interpret the various shut intervals as reflecting sojourns of the AChR in either closed or desensitized conformations, and because the number of channels in each patch was not known (the probability of an unliganded channel being open is so low that multiple channels may be gating at the same time without this being evident as overlapping openings), the interval between any two consecutive openings in a recording could not be ascribed any physical meaning. The distinction between channel sojourns in closed conformations and desensitized conformations (which can usually be made with currents from liganded receptors) is of fundamental importance because it is the closed-interval durations that are needed to estimate an opening rate constant.

Presented in this way, the complexity of unliganded AChR gating kinetics appears to be irreconcilable with the simple two-state reaction scheme that is required to characterize a transition state. However, a number of experimental observations point to the possibility that gating of unliganded AChRs can still be described by a two-state, closed $\rightleftharpoons$ open reaction scheme. First, diliganded gating can be kinetically modeled as a one-step reaction, so it is likely that its unliganded counterpart is a one-step process as well. Second, the shortest lived type of opening accounted for the majority of the recorded openings, so irrespective of the origin of the multiple exponential open components, the main properties of the unliganded open $\rightarrow$ closed reaction should be captured by the sole description of the briefest component of the open-

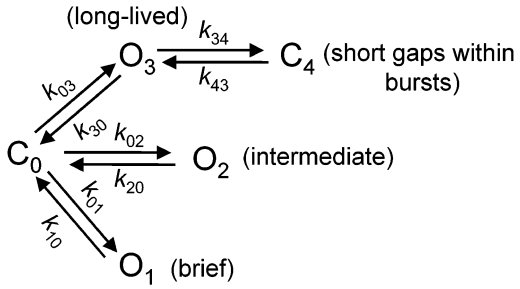

FIGURE 5: Example reaction scheme used to interpret unliganded AChR single-channel currents. The letters "C" and "O" denote nonconductive ("shut") and conductive ("open") conformations of the receptor channel, respectively. The number of states in the model depended on the extent to which their inclusion/omission affected the maximum log likelihood of the fit. Additional states were justified only if their inclusion increased this value by at least five units per state. The O_1 state was needed in all the recordings, whereas O_2 and O_3 were needed in only some of them. Additional shut states, which were needed in most experiments, were added to C_0 as a linear chain.

time distribution. With this in mind, I fitted the data (i.e., series of shut- and open-interval durations) to a kinetic scheme where the different types of openings are isolated from one another (Figure 5). In this way, the fastest (and main) closing rate constant is simply the reciprocal of the mean lifetime of the briefest open component, and the presence of additional open components can be easily disregarded. Figure 5 shows a particular example of this model, which was used to fit data that displayed the three types of openings (O_1, O_2, and O_3), the short gaps within bursts of long-lived openings (C_4), and only one more shut exponential component (C_0). Because of the ambiguities associated with the physical interpretation of shut intervals, only the closing (k_{10}, k_{20}, and k_{30}) and the intraburst (k_{34} and k_{43}) rate constants were used to analyze the effect of mutations. The k_{01}, k_{02}, and k_{03} rate constants were used only as ratios, to estimate the proportion of each type of opening.

Mutational Analysis. Since the aim of this study was to compare the transition-state structure in diliganded and unliganded AChRs, I decided to estimate the unliganded Φ-values in regions of the protein where, according to our previous studies (*8*, *10*−*12*), the closed ⇌ open allosteric transition of *diliganded* AChRs has progressed to different extents at the transition state. Thus, I chose residues at, or near, the transmitter-binding sites (αY93, αY190, and αD200), a residue in the M2−M3 linker (αS269), three residues in the extracellular half of M2 (12′ position, βT265, δS268, and εT264), and two residues in the middle of M2 (9′ position, αL251 and δL265).

Here, I compare these positions' Φ-values in unliganded receptors to those in AChRs diliganded with ACh (binding-site mutants) or the weak agonist choline (all other mutants). For each construct, and assuming that the effect of mutations and presence/absence of ligand are independent, the different "background" (i.e., unliganded versus diliganded) corresponds to a $\sim 10^7-10^8$-fold change in the gating equilibrium constant ($\Delta\Delta G^\circ \cong -10.0$ kcal/mol) when the ligand is ACh, and to a $\sim 10^4-10^5$-fold change ($\Delta\Delta G^\circ \cong -6.0$ kcal/mol) when the ligand is choline. The fact that the wild-type AChR's unliganded gating equilibrium constant is not known with accuracy (I am assuming here a value of 10^{-6}, on the basis of previous experimental data; *18*, *51*) adds some uncertainty to these calculated *n*-fold changes, but as we will see below, this does not compromise the conclusions at all.

Transmitter-Binding Sites. The transition state of unliganded gating was probed with three binding-site mutations (αY93F, αY190W, and αD200N) which, in addition to possible effects on the affinity of the receptor for the ligand, decrease the unliganded-gating equilibrium constant (*18*). Because the latter is already very small in the wild type, these mutations were engineered on the background of a gain-of-function construct that displays an increased unliganded activity: the M2 12′ double mutant δS268T + εT264S.

In recordings from the unliganded triple mutants (αY190W, αD200N, or αY93F on the double-mutant background), only the brief type of opening was observed. In the case of the background construct, both the brief and long-lived types were present, but the brief component accounted for as much as 86.4% of the total openings (*18*). The fastest closing rate constants, k_{10} (see Figure 5), of the triple mutants were 15855 ± 4588 s^{-1} (mean ± SE; $n = 3$ patches) for αY190W, 8157 ± 817 s^{-1} ($n = 5$) for αD200N, and 8483 ± 570 s^{-1} ($n = 4$) for αY93F, whereas that of the background construct was 10648 ± 583 s^{-1} ($n = 4$). An inspection of these rate constants suggests that the decreased unliganded activity caused by the three binding-site mutations must be due to a slower opening rate constant because the closing rate constant (k_{10}) changes very little, or even in the "wrong" direction, upon mutation. In terms of Φ-values, these results imply that $\Phi \cong 1$ for these three residues during unliganded gating. We have previously found that Φ is also ∼1 at, or near, the binding sites during diliganded gating (*11*). It can be concluded then that, regardless of whether the binding sites are liganded or unliganded, the conformational rearrangement of the transmitter-binding sites that occurs upon opening is almost complete at the transition state (or, from microscopic reversibility, that the conformational rearrangement of the transmitter-binding sites that occurs upon *closing* has not even started when the transition state is reached).

M2−*M3 Linker.* The transition state of unliganded gating was probed with one mutation (αS269I) that increases the diliganded-gating equilibrium constant by a factor of ∼90, having little, if any, effect on ligand-binding affinities (*10*). In the framework of the thermodynamic cycles that are used to interpret the function of allosteric proteins, this suggests that this mutation should increase the unliganded-gating equilibrium constant ∼90-fold as well. The increased unliganded activity caused by the αS269I mutation is exemplified in Figure 2.

The value of the fastest closing rate constant, k_{10}, was 11633 ± 426 s^{-1} (mean ± SE; $n = 7$ patches), and that of the background construct (wild type) was 12187 ± 1104 s^{-1} ($n = 5$). This suggests that the ∼90-fold increase in the unliganded-gating equilibrium constant must be due to a ∼90-fold faster unliganded opening rate constant because the closing rate constant hardly changes upon mutation ($\Phi \cong 0.99$). This contrasts with the situation during diliganded gating where the ∼90-fold increase in the equilibrium constant caused by this mutation is due to a ∼30-fold increase in the opening rate constant and a ∼3-fold decrease in the closing rate constant ($\Phi \cong 0.76$). Evidently, the structural rearrangement of the M2−M3 linker that accompanies the closed → open reaction has progressed to

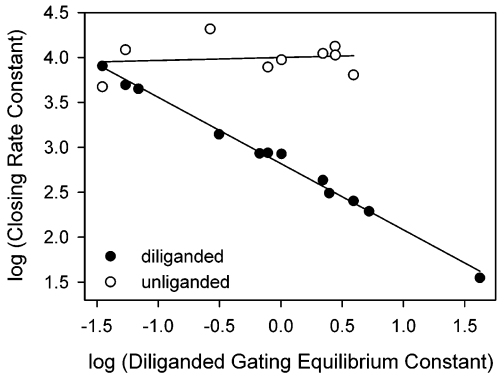

FIGURE 6: Rate−equilibrium plots of diliganded and unliganded gating for an M2 12′ mutant series. The slope of the choline-diliganded plot was −0.737 (Φ = slope + 1 = 0.263; *8*, *11*). The slope of the unliganded plot, however, was 0.033 (Φ = 1.033). Thus, the gating Φ-value at position M2 12′ depends on the occupancy status of the transmitter-binding sites.

different extents at the transition states of diliganded and unliganded gating.

M2. Diliganded-gating Φ-values define two domains in the M2 segment of the δ subunit (*12*). The extracellular half of this 19-residue segment has an average Φ-value of 0.32 ± 0.03 (mean ± SE; four positions tested, 12′, 13′, 17′, and 19′), whereas the intracellular half has an average Φ-value of −0.07 ± 0.03 (five positions tested, 2′, 5′, 7′, 9′, and 10′), suggesting that the rearrangement of the extracellular half precedes that of the intracellular half in the closed → open direction. To compare the transitions states of diliganded and unliganded AChR gating in this pore-lining transmembrane segment, I performed a Φ-value analysis of unliganded gating at positions 12′ (extracellular half) and 9′ (intracellular half).

The Φ-value analysis at M2 12′ was performed using a series of mutations, which allows the presentation of the data in the form of rate−equilibrium plots (Figure 6). M2 12′ mutations increase the diliganded (*8*) and unliganded (*18*) gating equilibrium constants, and the effect on ligand-binding affinities appears to be negligible. This implies that the *change* in the unliganded-gating equilibrium constant caused by any of the 12′ mutations used here should be very close (identical actually, if the binding affinities were completely unaffected) to the change caused by the same mutation in the diliganded equilibrium constant. This concept is an important one because it allowed me to plot the rate−equilibrium plots of *both* diliganded and unliganded gating using the (log of the) diliganded-gating equilibrium constant in the *x*-axis (unlike that of diliganded gating, the equilibrium constant of unliganded gating could not be estimated experimentally because of the uncertainties associated with the physical interpretation of shut intervals noted above). Since it was the closing rate constants (and not the opening rate constants) of unliganded gating that were determined experimentally, unliganded and diliganded closing rate constants were used in the *y*-axis of the rate−equilibrium plot, and hence, Φ = 1 + slope. The "diliganded plot", which has been previously described (*11*), includes data from 12 different constructs differing only in the amino acid residue at position δ12′, and it is used here for comparison with the "unliganded plot". The latter includes data from the wild-type construct, δ12′ mutants (δS268A, T, I, Y, and N), a β12′ mutant (βT265S), a β12′ + δ12′ double mutant (βT265S + δS268T), and a δ12′ + ε12′ double mutant (δS268T + εT264S). The unliganded-gating Φ-value turns out to be ∼1.03, implying that changes in the equilibrium constant upon mutation are mostly due to changes in the opening rate constant, and suggesting that this portion of M2 experiences an "open-state-like" environment at the transition state of unliganded gating. As is the case for the M2−M3 linker, the M2 12′ unliganded Φ-value differs from the diliganded value, but in this case, the difference is larger (diliganded δ12′ Φ ≅ 0.26).

To probe the intracellular half of M2, I studied a mutation at the δ9′ position (δL265T). In previous studies (*12*), we found that this mutation increases the diliganded-gating equilibrium constant by a factor of ∼23, and here I show that this mutation increases unliganded gating as well (Figure 3). The fastest closing rate constant, k_{10}, was 8142 ± 858 s^{-1} (mean ± SE; $n = 3$ patches), which represents a modest ∼1.5-fold decrease from the wild-type value of 12187 s^{-1}. This implies that the increased unliganded activity of this δ9′ mutant is mostly due to a faster unliganded opening rate constant. Indeed, calculation of the Φ-value assuming that the unliganded equilibrium constant also increases by a factor of 23 yields Φ ≅ 0.87. This suggests that, like the other AChR domains probed (transmitter-binding sites, M2−M3 linker, and the extracellular half of M2), this portion of M2 experiences an open-state-like environment at the transition state of unliganded gating. This is in stark contrast with the situation during diliganded gating, where the ∼23-fold increase in the equilibrium constant caused by the δL265T mutation is almost entirely due to a slower closing rate constant (Φ ≅ 0.03).

Analysis of the effect of a mutation in the 9′ position of the α subunit (αL251A) lends further support to the notion of a late transition state for the unliganded gating reaction. This mutation increases the unliganded activity, and the fastest closing rate constant, k_{10}, was 8191 ± 657 s^{-1} (mean ± SE; $n = 3$ patches). This also represents a small decrease (<1.5-fold) from the wild-type value. This implies that the increased unliganded activity of this α9′ mutant is mostly due to a faster unliganded opening rate constant and, hence, that Φ should be close to 1, as for all the other residues probed. The increased unliganded activity caused by this mutation is exemplified in Figure 4.

To calculate all the Φ-values above, I have assumed that the AChR's unliganded-gating equilibrium constant (which could not be determined experimentally) changes upon mutation by the same factor as the diliganded-gating equilibrium constant (which *could* be determined). In fact, that this may indeed be the case was only tested in a few of the mutants studied here (*6*, *8*), so this assumption is a generalization of a limited observation. In any case, the effect of mutations on the unliganded activity was so obvious that even if this assumption were not quantitatively exact for all the constructs, it is clear that the gating equilibrium constant of unliganded AChRs decreases in the binding-site mutants, and increases in the M2−M3-linker and M2 mutants. Also, it is clear from the data that the "main" closing rate constant of the unliganded receptor remains close to the background value (∼10000 s^{-1}) upon mutation. Thus, even a qualitative analysis of these observations suggests that the transition state of unliganded gating looks much like the open state.

Actual Limit or Technical Limitation? The results indicate that the unliganded closing rate constant remains roughly the same (∼10000 s^{-1}) upon mutations and, hence, that the opening rate constant must be "absorbing" all the changes in the equilibrium constant. Because the ability to estimate a rate constant correctly is expected to decrease as the rate constant becomes faster, it seemed prudent to ask whether the limit of ∼10000 s^{-1} represents an actual property of the muscle AChR or, simply, a technical limitation. To address this point, I simulated single-channel currents using a closed ⇌ open kinetic scheme under conditions that reproduce my experimental settings (a dead time of 25 μs, a sampling rate of 100 kHz, a bandwidth of 20 kHz, a signal of ∼6 pA, and a root-mean-square noise of ∼1.6 pA for the open channel and of ∼1.5 pA for the closed channel, both measured with a 20 kHz bandwidth) and with a variable closing rate constant. Kinetic analysis of the simulated data, following exactly the same procedures as for experimental recordings, yielded the relationship shown in Figure 7. It can be concluded from this figure that the value of ∼10000 s^{-1} is well in the region where rate constants are estimated correctly, and that faster values, had they occurred, could have been detected with considerable accuracy at least up to ∼75000 s^{-1} (in which case the ratio between the estimated and simulated rate constants is ∼0.9). It seems that the closing rate constant of muscle AChRs cannot be made much faster than ∼10000 s^{-1}, at least by the type of perturbations used in this paper. It is perhaps worth noting here that the closing rate constant of ACh-diliganded or choline-diliganded AChRs is in the 2000−3000 s^{-1} range.

Single-Channel versus Ensemble Measurements. If single-channel measurements are made, then the forward and backward rate constants of one-step gating reactions can be estimated separately. This leads to rate−equilibrium plots that are linear, and to Φ-values that are related to the slopes of these plots in a trivial manner. This is, for example, the case of choline-diliganded AChRs. A variety of other ion channels, however, cannot be studied at the single-molecule level because their single-channel conductances are exceedingly low (among neurotransmitter-gated ion channels, this is the case for serotonin type 3A, and γ-aminobutyric acid type C receptors, for example). Instead, these channels have to be studied at the macroscopic or "ensemble" level, with the (apparent) disadvantage that the opening and closing rate constants cannot be estimated separately. What would rate−equilibrium plots look like in this case? Could Φ-values still be extracted from the macroscopic data? Figure 8 illustrates the simple case where the opening and closing rate constants can only be estimated as their sum, as would be the case if the macroscopic current through a neurotransmitter-activated ion channel that gates with two-state kinetics were measured upon rapidly stepping the concentration of agonist from zero to saturating. The figure plots what would be the "observed macroscopic opening rate" (or, rather, the reciprocal of the time constant of the monoexponential current rise) as a function of the gating equilibrium constant for different Φ-values. Although these plots of log(rate) versus log(equilibrium constant) are not straight lines, as they would be if the opening and closing rate constants could be estimated separately, Φ-values can still be easily obtained by fitting the underlying function. The conclusion is that, as long as the mathematical relationship between the observed macroscopic time constant and the individual rate constants is known, Φ-values can be estimated, and single-channel measurements are not imperative. Indeed, this is the case for Φ-value studies in the context of protein folding, which usually do not involve single-molecule measurements, and where the folding and unfolding rate constants can only be estimated as their sum. Not surprisingly, "slices" of the 3-D plot in Figure 8, perpendicular to the Φ-value axis, are reminiscent of the V-shaped *chevron* plots of two-state protein folding.

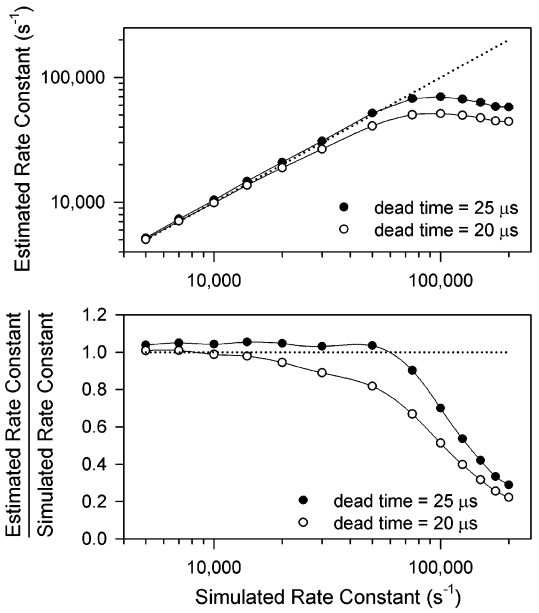

FIGURE 7: Relationship between simulated and estimated rate constants. To mimic the experimentally recorded unliganded AChR data, single-channel currents were simulated using a two-state, closed ⇌ open kinetic scheme with QuB software. To determine how accurate the estimates of the fastest closing rate constant are, the opening rate constant was fixed at an arbitrary value of 500 s^{-1}, whereas the closing rate constant was varied from 5000 to 200000 s^{-1}. The single-channel current amplitude (6.0 pA) and the root-mean-square noise of the closed (1.5 pA; 20 kHz bandwidth) and open (1.6 pA; 20 kHz bandwidth) current levels were set to values similar to those recorded experimentally. Simulated currents were idealized (20 kHz bandwidth) using the SKM algorithm, and the corresponding rate constants were estimated using the MIL algorithm, both in QuB software. Each point in the plot represents the average of five rate-constant estimates, each resulting from an independent simulation. In turn, each rate-constant estimate was the result of the analysis of the same number of open/shut intervals (5000 after the imposition of a dead time). Hence, the deviation from the ideal relationship (dotted lines in both plots) cannot be ascribed to differences in the number of intervals analyzed. The shape of these plots is very sensitive to a number of variables, including the signal-to-noise ratio of the current recordings, the rate at which the currents were digitized, the bandwidth used for idealization, and the dead time imposed on the idealized data before the estimation of rate constants (the latter is explicitly illustrated in the figure; the experimentally recorded data were analyzed with a value of 25 μs). Therefore, these plots should not be regarded as a general property of the algorithms implemented in the software but merely as an indication of the accuracy with which rate constants were estimated in this particular paper.

DISCUSSION

The finding that mutations at the transmitter-binding sites affect the gating equilibrium constant of unliganded channels (*18*) strongly supports the notion that the low- to high-affinity change at the binding sites occurs upon gating even if these

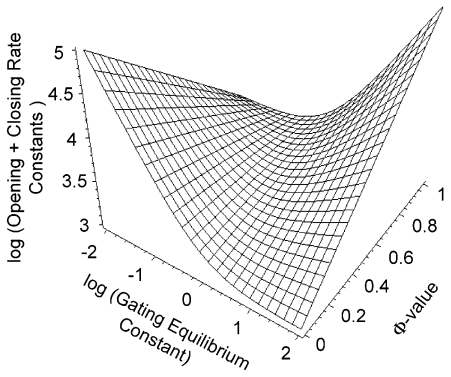

FIGURE 8: Simulation of rate−equilibrium plots at different Φ-values in the case where the forward and backward rate constants of a one-step reaction can only be estimated as their sum. The intrinsic opening and closing rate constant (i.e., the value of these rate constants when the equilibrium constant is equal to 1; see eqs 2 and 3 in the Experimental Procedures) was arbitrarily set at 1000 s^{-1}. The particular value of this rate constant does not affect the shape of this plot; it simply shifts it up or down.

are not occupied by cholinergic ligands. Also, the fact that the conductances of liganded and unliganded AChRs are indistinguishable suggests that the conformations of the ion pathway in the closed and open states are oblivious to the presence or absence of ligand in the binding sites. It follows, then, that the molecular rearrangements that take place during gating are likely to be very similar regardless of whether the receptor channel is diliganded or unliganded.

But can we say anything about their *mechanisms*? If we defined "mechanism" as the entire sequence of transient conformations that the AChR adopts in going from the closed to the open state, and vice versa (the conformations are the same in either direction; only the order in which they occur is reversed), then what can be said is limited. The best that can be done to address the issue of mechanisms, at least for the time being, is to characterize the conformation of the transition state, and the only way of doing this is by analyzing the reaction's kinetics in the framework of the linear free-energy relationships of physical organic chemistry (*13*, *14*). Of course, because the "transition state" is just one or, rather, a few conformations along the reaction pathway, the underlying continuous mechanism is not uniquely determined by even the most thorough Φ-value analysis, but at least it becomes firmly "anchored".

The results presented here indicate that the transition state of gating is very different in diliganded and unliganded AChRs. In the former case, the transition state is somewhat polarized, with regions that are closed-state-like, regions that are open-state-like, and regions that lie somewhere in between. In the case of unliganded gating, in contrast, all the residues that were probed with mutagenesis (this paper) and the transmembrane-voltage-sensing domains (*11*, *18*) have open-state-like environments at the transition state. Accordingly, the structure of the transition state inferred from the unliganded Φ-values casts no light on the intermediate stages of this allosteric transition, let alone on its mechanism. Thus, the question of whether opening of unliganded AChRs proceeds through the same sequence of conformational changes as opening of diliganded AChRs (that is, initiating at the transmitter-binding sites and propagating toward the intracellular end of the pore domain), or even whether the unliganded conformational change propagates at all, instead of taking place in a synchronous manner, cannot be answered.

Changes in the position of the transition state on a reaction's energy landscape are very well documented in organic chemistry and in protein-folding studies, and can be rationalized in a number of ways. One such way is known as the "Hammond/anti-Hammond postulate" (*20*−*22*, *24*, *25*, *52*), which posits that the transition state passively "slides" on a perturbed energy landscape until it "finds" its new location. The magnitude and direction of this displacement depend on a variety of factors that include the extent of the energy-landscape deformation, the steepness of the free-energy surface in the vicinity of the transition state, and the specific region of the landscape being deformed. Consequently, the mere fact that two different perturbations change the equilibrium constant of a reaction by the same factor does not imply that they will move the transition state to the same new location, or that the reaction's Φ-values will all be shifted in the same direction and by the same amount. If we describe the displacement of the transition state as a vector, then its projection on an axis parallel to the reaction pathway is usually referred to as a Hammond type of movement, while the projection perpendicular to the reaction pathway is referred to as anti-Hammond. Movement along (parallel to) the reaction pathway occurs in such a way that the transition state slides away from the stabilized region of the landscape, whereas movement in the perpendicular direction occurs toward the stabilized region (*24*, *25*). Thus, the shift in Φ-values observed when unliganded and diliganded AChR gatings are compared (all probed Φ-values become ∼1 in unliganded receptors) is consistent with the displacement of the transition state *along* the reaction pathway, away from the more stabilized end state. This result is in accord with the main prediction of the Hammond postulate (*20*), namely, that *all* parts of the reacting molecule should become more product-like as the products are destabilized relative to the reactants. This prediction follows from the ideas that a ground state cannot be made more unstable than the transition state itself, and that the closer two species are in free energy, the closer they are in structure, as well. If the Hammond phenomenon were indeed the basis of the observed transition-state movement, then the mechanism of gating would be largely preserved. In other words, gating of unliganded AChRs would proceed through a very similar cascade of molecular rearrangements as diliganded gating because the transition state would stay *on* the reaction pathway (or, more realistically, very close to it) as it slides. It is clear that the Hammond/anti-Hammond postulate is essentially correct, and that the predicted movements of the transition state *must* necessarily occur in response to the deformation of the free-energy surface. What is not clear, however, is the extent to which this phenomenon accounts for the experimentally observed changes in transition-state Φ-values. A Hammond-postulate behavior has been invoked frequently (e.g., refs *27*, *30*, *32*, and *53*−*58*), perhaps improperly in many cases (*23*, *52*, *59*, *60*), in the context of organic-chemistry and protein-folding reactions.

Another plausible scenario that can account for changes in the position of the transition state is based on the idea that two or more (instead of only one) sequential barriers may actually exist along the pathway of reactions with two-state kinetics, provided that only one of the transition states

dominates the kinetics at any single time. The deformation of the energy landscape upon perturbation would, then, cause the alternative exposure of the different transition states, thus accounting for the observed changes in Φ-values. The shift in Φ-values observed when unliganded and diliganded AChR gatings are compared is also consistent with this model. The kinetics of diliganded gating would be dominated by one transition state, and those of unliganded gating by a later one (occurring closer to the open state), the switch between them being caused by the tilt produced in the free-energy landscape in going from diliganded receptor to unliganded receptor gating. This model could be referred to as "a change in the rate-limiting step", and as long as the number of sequential barriers is not too large, it could be regarded as a sort of discrete version of the Hammond postulate, with the alternative transition states also lying roughly on the same reaction pathway. Although in principle the two models make different predictions as to the changes in Φ-values (a continuous change in the Hammond model, and a change between a few discrete values in the sequential-barrier model), identifying which one fits the experimental observations best is far from unambiguous, even when the experimental data are plentiful (*60*). In the present case, analyzing only "two points" (the unliganded and diliganded situations), these two models cannot be distinguished.

A third possibility is somehow related to the "change-in-rate-limiting-step" model discussed above, but here, the alternatively exposed transition states would lie on completely different reaction pathways. Accordingly, this scenario could be referred to as "a change in the reaction mechanism". This type of model is often invoked in studies of protein folding (e.g., refs *29*, *34*, *61*, and *62*) to account for those cases where changes in Φ-values upon perturbation do not follow a monotonic pattern (some Φ-values increase; others decrease) and occur abruptly, between two discrete sets of values. In our case, it is impossible to rule out that unliganded and diliganded AChR gatings proceed through completely different mechanisms; the transition state lies so close to the open state that all information about intermediate stages in the reaction is lost.

Yet another, quite different, way of rationalizing changes in Φ-values upon experimental perturbations has been recently proposed. In an analysis of existing protein-folding experimental data, Sánchez and Kiefhaber (*59*) concluded that changes in the structure of the end states, rather than the usually invoked changes in the structure of the transition state itself, can account for the observed changes in Φ-values. In the particular case of the AChR, for example, the unliganded-gating transition state could look more open-like simply because the structure of the unliganded open state has changed, becoming more similar to that of the transition state, and not because of a change in the structure of the transition state. Because Φ-values are a *relative* measure of structure (relative to the end states), the data presented here do not allow us to tell whether it is the transition state that "moves" toward the open state or whether it is the open state that changes, approaching the transition state. In any case, it is clear that the transition state and the open state become closer upon the diliganded → unliganded perturbation.

Choosing among these different scenarios to interpret the experimental data is not trivial. This is because the predictions of the different models overlap to some extent, and because it is almost impossible to obtain data under the extreme experimental conditions that need to be probed to allow a clear distinction. Indeed, quite different interpretations for exactly the same set of experimental observations can be found in the literature of protein folding (*59*, *60*). It is also likely that elements of the four scenarios discussed above (and perhaps of others as well) are present together during "real" transition-state movements. Irrespective of the precise phenomenon underlying the relocation of the transition state on the energy landscape, however, the changes in Φ-values reported here reveal that ion-channel gating landscapes are malleable multidimensional energy surfaces. This is the central conclusion of this paper.

An implication of a transition state lying very close to one of the end states is that the activation barrier that needs to be surmounted to leave that state is the lowest possible. This happens because the end state and the transition state are so similar that any further destabilization of the end state is accompanied by an identical destabilization of the transition state, and therefore, the height of this residual activation barrier remains constant. If, as suggested by the experimental data presented here, $\Phi \cong 1$ in all regions of the unliganded AChR, then it is likely that the closing rate constant of the muscle AChR (be it diliganded or unliganded, mutant or wild type) cannot be made much faster than $\sim$10000 s^{-1}, the value consistently found for the unliganded closing rate constant of wild-type and mutant AChRs. This is in sharp contrast with the opening rate constant, which is as fast as $\sim$50000 s^{-1} in ACh-diliganded wild-type receptors, and can probably be sped up beyond that by mutations (*10*).

Finally, the fact that the location of the transition state on the gating free-energy landscape of choline-diliganded AChRs differs from that in unliganded receptors suggests that the structure of the transition state in the presence of choline might also be different from that in the presence of other agonists. Thus, it is not a foregone conclusion that choline Φ-values can be used to interpret results in the presence of ACh, for example. This is an important limitation because the fast gating kinetics of receptors diliganded with ACh usually render the experimental estimation of Φ_{ACh}-values extremely difficult (*8*).

It would be interesting to know whether the malleability of the gating energy landscape evinced by these experiments with the muscle AChR is a particular feature of this type of channel or a property of the physical chemistry of ion-channel gating in general. To the extent that single-channel measurements are not needed (as exemplified in Figure 8), and that ion channels other than the AChR also display two-state gating kinetics, this issue could be explored experimentally.

ACKNOWLEDGMENT

I thank Anthony Auerbach for discussions and support during the initial stages of this project. I also thank Steven Sine for the generous gift of AChR cDNAs.

REFERENCES

1. Edmonds, B., Gibb, A. J., and Colquhoun, D. (1995) *Annu. Rev. Physiol. 57*, 469−493.
2. Karlin, A. (2002) *Nat. Rev. Neurosci. 3*, 102−114.
3. Karlin, A. (1967) *J. Theor. Biol. 16*, 306−320.

4. Jackson, M. B. (1989) *Proc. Natl. Acad. Sci. U.S.A. 86*, 2199−2203.
5. Edelstein, S. J., and Changeux, J.-P. (1998) *Adv. Protein Chem. 51*, 121−184.
6. Grosman, C., and Auerbach, A. (2001) *Proc. Natl. Acad. Sci. U.S.A. 98*, 14102−14107.
7. Valenzuela, C. F., Weign, P., Yguerabide, J., and Johnson, D. A. (1994) *Biophys. J. 66*, 674−682.
8. Grosman C., and Auerbach, A. (2000*a*) *J. Gen. Physiol. 115*, 637−651.
9. Bernasconi, C. F. (1985) *Tetrahedron 41*, 3219−3234.
10. Grosman, C., Salamone, F. N., Sine, S. M., and Auerbach, A. (2000) *J. Gen. Physiol. 116*, 327−340.
11. Grosman, C., Zhou M., and Auerbach, A. (2000) *Nature 403*, 773−776.
12. Cymes, G. D., Grosman, C., and Auerbach, A. (2002) *Biochemistry 41*, 5548−5555.
13. Leffler, J. E. (1953) *Science 117*, 340−341.
14. Leffler, J. E., and Grunwald, E. (1963) *Rates and Equilibria of Organic Reactions*, John Wiley and Sons, New York.
15. Brönsted, J. N., and Pedersen, K. (1924) *Z. Phys. Chem. 108*, 185−235.
16. Fersht, A. R., Leatherbarrow, R. J., and Wells, T. N. C. (1986) *Nature 322*, 284−286.
17. Auerbach, A., Sigurdson, W., Chen, J., and Akk, A. (1996) *J. Physiol. 494*, 155−170.
18. Grosman C., and Auerbach, A. (2000*b*) *J. Gen. Physiol. 115*, 621−635.
19. Leite, J. F., and Cascio, M. (2002) *Biochemistry 41*, 6140−6148.
20. Hammond, G. S. (1955) *J. Am. Chem. Soc. 77*, 334−338.
21. Thornton, E. (1967) *J. Am. Chem. Soc. 89*, 2915−2927.
22. Mok, M. H., and Polanyi, J. C. (1969) *J. Chem. Phys. 51*, 1451−1469.
23. Jencks, W. P., Brant, S. R., Gandler, J. R., Fendrich, G., and Nakamura, C. (1982) *J. Am. Chem. Soc. 104*, 7045−7051.
24. Jencks, W. P. (1985) *Chem. Rev. 85*, 511−527.
25. Jencks, W. P. (1988) *Bull. Soc. Chim. Fr. 2*, 218−224.
26. Lopez, X., Dejaegere, A., and Karplus, M. (2001) *J. Am. Chem. Soc. 123*, 11755−11763.
27. Matouschek, A., and Fersht A. R. (1993) *Proc. Natl. Acad. Sci. U.S.A. 90*, 7814−7818.
28. Burton, R. E., Huang, G. S., Daugherty, M. A., Fullbright, P. W., and Oas, T. G. (1996) *J. Mol. Biol. 263*, 311−322.
29. Viguera, A. R., Serrano, L., and Wilmanns, M. (1996) *Nat. Struct. Biol. 3*, 874−880.
30. Daggett, V., Li, A., and Fersht, A. R. (1998) *J. Am. Chem. Soc. 120*, 12740−12754.
31. Oliveberg, M., Tan, Y.-J., Silow, M., and Fersht, A. R. (1998) *J. Mol. Biol. 277*, 933−943.
32. Crane, J. C., Koepf, E. K., Kelly, J. W., and Gruebele, M. (2000) *J. Mol. Biol. 298*, 283−292.
33. Pappenberger, G., Saudan, C., Becker, M., Merbach, A. E., and Kiefhaber, T. (2000) *Proc. Natl. Acad. Sci. U.S.A. 97*, 17−22.
34. Nauli, S., Kuhlman, B., and Baker, D. (2001) *Nat. Struct. Biol. 8*, 602−605.
35. Sine, S. M. (1993) *Proc. Natl. Acad. Sci. U.S.A. 90*, 9436−9440.
36. Salamone, F. N., Zhou, M., and Auerbach, A. (1999) *J. Physiol. 516*, 315−330.
37. Higuchi R. (1990) Recombinant PCR, in *PCR Protocols* (Innis, M. A., Gelfand, D. H., Sninsky, J. J., and White, T. J., Eds.) pp 177−183, Academic Press, San Diego.
38. Hamill, O. P., Marty, A., Neher, E., Sakmann, B., and Sigworth, F. J. (1981) *Pflügers Arch. 391*, 85−100.
39. Qin, F., Auerbach, A., and Sachs, F. (1996) *Biophys. J. 70*, 264−280.
40. Rabiner L. R., Wilpon, J. G., and Juang, B. H. (1986) *AT & T Technol. J. 65*, 21−31.
41. Li, L., and Shakhnovich, E. I. (2001) *Proc. Natl. Acad. Sci. U.S.A. 98*, 13014−13018.
42. Jaffé, H. H. (1953) *Chem. Rev. 53*, 191−261.
43. Klinman, J. P. (1976) *Biochemistry 15*, 2018−2026.
44. Matouschek, A., Kellis, J. T., Serrano, L., and Fersht, A. R. (1989) *Nature 340*, 122−126.
45. Eaton, W. A., Henry, E. R., and Hofrichter, J. (1991) *Proc. Natl. Acad. Sci. U.S.A.* 88, 4472−4475.
46. Yifrach, O., and Horovitz, A. (1998) *J. Am. Chem. Soc. 120*, 13262−13263.
47. Horovitz, A., Amir, A., Danziger, O., and Kafri, G. (2002) *Proc. Natl. Acad. Sci. U.S.A. 99*, 14095−14097.
48. Maglott, E. J., Goodwin, J. T., and Glick, G. D. (1999) *J. Am. Chem. Soc. 121*, 7461−7462.
49. Itzhaki, L. S., Otzen, D. E., and Fersht, A. R. (1995) *J. Mol. Biol. 254*, 260−288.
50. Colquhoun, D., and Sakmann, B. (1985) *J. Physiol. 369*, 501−557.
51. Jackson, M. B. (1986) *Biophys. J. 49*, 663−672.
52. Fărcasiu, D. (1975) *J. Chem. Educ. 52*, 76−79.
53. Matouschek, A., Otzen, D. E., Itzhaki, L. S., Jackson, S. E., and Fersht, A. R. (1995) *Biochemistry 34*, 13656−13662.
54. Matthews, J. M. and Fersht, A. R. (1995) *Biochemistry 34*, 6805−6814.
55. Silow, M. and Oliveberg, M. (1997) *Biochemistry 36*, 7633−7637.
56. Dalby, P. A., Oliveberg, M., and Fersht, A. R. (1998) *Biochemistry 37*, 4674−4679.
57. Otzen, D. E., Kristensen, O., Proctor, M., and Oliveberg, M. (1999) *Biochemistry 38*, 6499−6511.
58. Otzen, D. E., and Oliveberg, M. (2002) *J. Mol. Biol. 317*, 613−627.
59. Sánchez, I. E., and Kiefhaber, T. (2003*a*) *J. Mol. Biol. 327*, 867−884.
60. Sánchez, I. E., and Kiefhaber, T. (2003*b*) *J. Mol. Biol. 325*, 367−376.
61. Kuhlman, B., O'Neill, J. W., Kim, D. E., Zhang, K. Y., and Baker, D. (2002) *J. Mol. Biol. 315*, 471−477.
62. Lindberg. M., Tångrot, J., and Oliveberg, M. (2002) *Nat. Struct. Biol. 9*, 818−822.

BI0354334